JOURNAL OF PROPULSION AND POWER
Vol. 13, No. 6, November–December 1997

Effects of Inlet Configuration on Ignition and Fuel Regression Behind a Backstep

Cliff Yuh-Yih Wu* and Jing-Tang Yang†
National Tsing Hua University, Hsinchu, Taiwan 30043, Republic of China
and
Horng-Tsann Yang‡
Lung-Tan, Tao Yuan, Taiwan, Republic of China

Five step configurations were designed to investigate the effects of inlet step configurations on the flow structure and ignition of solid fuel behind a backstep. Experiments were conducted separately in a cold flow for the flowfield measurement and in a hot flow for the fuel regression before ignition and ignition tests. The step height was fixed at 29 mm for each configuration. The inlet velocity of the cold flow was 15 m/s. The velocity flowfield was measured with a laser Doppler anemometer and the ignition process was observed with a video camera. The configuration of the inlet step significantly affected the turbulence intensity of the shear layer and the reverse flow rate of the recirculation zone. The greater reverse flow rate provided a better flameholding capability, and hence, abbreviated the ignition delay. As the flow was turbulent, the higher the turbulence intensity and the longer the ignition delay. When the oxygen concentration was higher than 19%, the effect of inlet configuration on ignition diminished.

I. Introduction

THE backward-facing step is a fundamental element of the inlet port of many sudden-expansion combustors. The airstream over a backward-facing step produces a separating and reattaching flow containing a recirculation zone and a shear layer. Such a flow pattern is intimately related to the characteristics of ignition and flame stabilization. Extensive work on the flowfield behind a backstep has been performed: Etheridge and Kemp[1] conducted a detailed measurement of the flowfield and Eaton and Johnston[2] summarized the factors influencing the reattachment length. In addition, the flow structure is sensitive to the separation point of the backstep. Isomoto and Honami[3] discovered that turbulence intensity in the boundary layer at the separation point, rather than in the freestream, was a significant parameter governing reattachment length.

The flowfield behind a backward-facing step significantly affects mass transfer and heat transfer and, hence, flame stabilization. Vogel and Eaton[4] studied the heat transfer of cold flow over a backstep with a constant heat flux at the wall, and found that the maximum heat transfer was located in the reattachment region. Sirka et al.[5] reported that the mechanism of heat transfer in the wake flow was significantly affected by the flow pattern. Kundu et al.[6] emphasized that the transport of mass and heat between the main stream and the recirculation zone was proportional to the maximum reverse flow rate. Yang et al.[7] reported that the flow features that stabilize the flame abbreviated the ignition delay.

A backstep is generally used in the solid fuel ramjet (SFRJ) to provide flame stabilization. Korting et al.[8] observed that the combustion process started in the recirculation zone and proceeded gradually downstream in the fuel grain. Elands et al.[9] defined the flammability as the combustion partially sustained in the recirculation zone, and reported that an increase in A_p/A_t (port-to-throat area ratio) as well as in A_p/A_{in} (port-to-inlet area ratio) would enhance the flammability. Mixing between fuel vapor and air is important for ignition and combustion. Schadow et al.[10] stated that mixing between the fuel-rich and air-rich regions had to be accomplished to achieve high combustion efficiency. In their study of the effects of mass injection from the bottom wall behind the step on the reattaching flow, Richardson et al.[11] stated that the recirculation zone was well stirred at a low injection rate. Schulte et al.[12] measured the temperature and concentration in an SFRJ combustor, and reported that the recirculation zone was not a homogeneous well-stirred region, but was fuel rich. In the recirculation zone, the combustion process took place mainly in the shear layer of the incoming airflow.

Previous work has indicated that features of flow and combustion are sensitive to the geometric shape of the backstep. It is thus worthwhile to investigate an improved backstep configuration with favorable characteristics of ignition and flame stabilization characteristics. The objective of this work was to study the effects of configuration at the inlet of a combustor on the ignition of a solid fuel by varying five geometric backstep shapes. The experimental works included cold gas flow measurements, ignition tests, and the local regression of solid fuel before ignition. The results of this study will provide information about the interactions between flow structure and ignition.

II. Experimental Design

A. Test Rig

A schematic diagram of the wind tunnel and experimental setup appears in Fig. 1. Experiments were conducted in an open-circuit wind tunnel equipped with a 75-kW Roots blower, with speed controlled by a frequency inverter. The blower provided a maximum flow rate of 50 m^3/min. The fluid in the test section was either cold (for measurement of the flowfield) or hot (for regression and ignition tests). The hot oxidizing flow was generated by burning liquefied petroleum gas (LPG) composed of 50% propane and 50% butane, with air in a specially designed vitiator. The gas temperature was controlled by altering the flow rate of LPG, and the oxygen concentration was varied by adding gaseous oxygen to the air. A divergent sec-

Received July 26, 1994; revision received Nov. 1, 1994; accepted for publication Jan. 17, 1995.

*Ph.D. Candidate, Department of Power Mechanical Engineering.
†Professor, Department of Power Mechanical Engineering. Member AIAA.
‡Senior Specialist, P.O. Box 90008-15-1.

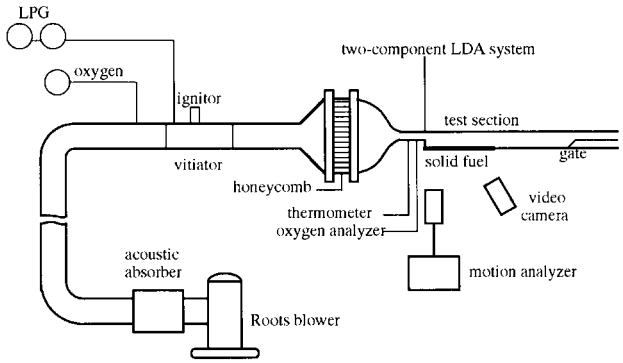

Fig. 1 Schematic diagram of experimental apparatus.

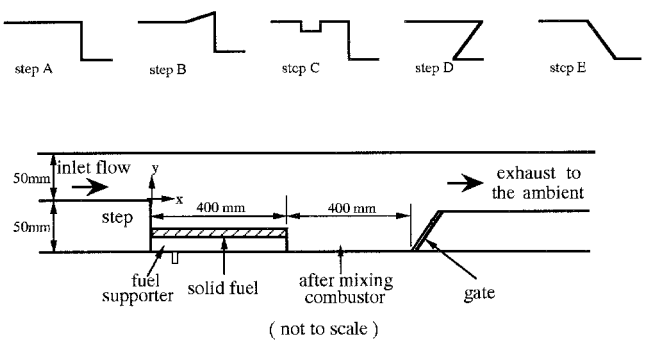

Fig. 2 Configurations of five steps and dimensions of test section.

tion, a settling chamber with a stainless-steel honeycomb, and a convergent section with a contraction ratio of 13.6 ahead of the test section reduced the turbulence level of the flow.

The configurations of five backsteps and a schematic diagram of the test section are presented in Fig. 2. Step A is the traditional backstep, and steps B, C, D, and E are modified. The step heights in all cases were 29 mm, and the aspect ratio (channel width to step height) was 6.9. The cross section of the combustor inlet was 50 mm high by 200 mm wide. A quartz window was installed on one side wall of the combustor to measure the flowfield and to visualize the ignition process. A polymethylmethacrylate (PMMA) slab (10 mm thick, 400 mm long, and 110 mm wide) was used as the fuel. The properties of the PMMA slab[13] are as follows: density, 1.19 g/cm^3; specific heat, 2.1 J/(gK); thermal conductivity, 0.0027 J/(cm s K); vaporization temperature, 668 K; effective heat of vaporization, 1.6 kJ/g-fuel; heat of reaction, 13.5 kJ/g-oxidant; and activation energy, 151 kJ/mol. The slab was laid in the center of a steel supporter 400 mm long and 196 mm wide. The bottom and two sides of the fuel slab were insulated.

B. Instrumentation

The cold gas flowfield was measured with a three-beam, two-color laser-Doppler anemometer (LDA). The LDA system was connected to a computer-controlled traversing system for two-dimensional movement. The resolution of the traverse system was 0.03 mm. The focusing and receiving optics of the LDA system were mounted on an optical bench that was placed on a traverse table to enable major movements.

The 514.5- and 488-nm wavelength beams of an argon-ion laser (5 W) were used to produce two LDA fringe patterns. The optical probe volume size was about 0.13 mm in diameter and 1.7 mm long, based on the $1/e^2$ intensity points in the spanwise direction. Each of the two pairs of beams had one beam Bragg-shifted by 40 MHz to eliminate ambiguity of flow direction. Backward-scattered light from particles passing through the measuring volume was detected with two photomultiplier tubes. The signals from the photomultiplier tubes were processed with a coincidence filter and two counter processors. The seeding particles were generated with a TSI 9306 jet atomizer and introduced into the airstream at the contraction section in the wind tunnel. The seeding particles (diameter of the order of 1 mm) were made of 25% glycerin resolvent and a water solvent.

For the regression and ignition tests, the inlet velocity was measured with a pitot tube. The temperature of the inlet gas was measured with a K-type thermocouple and a digital thermometer (Fluke 2190A). The concentration of oxygen was measured with an oxygen analyzer (Signal model 8000). All inlet conditions were monitored just before the entrance of the combustion chamber. The ignition delay was recorded with a video camera (Sony CCD-340) at 30 photographs per second, and the ignition process with a motion analyzer (Kodak) with speed set at 2000 photographs per second.

C. Experimental Conditions and Data Accuracy

The flowfield was measured at ambient temperature (22 ± 3°C) and pressure with inlet flow velocity at 15 m/s; the Reynolds number based on the step height was 27,700. At each measuring point 2048 measurements were normally made. The corresponding maximum uncertainties were 3.2% for mean axial velocity, 4.9% for mean normal velocity, and 4.9% for turbulence intensity at the 95% confidence level. The corresponding maximum uncertainty of Reynolds shear stress was 13%.

The ignition test was carried out under a hot oxidizing flow stream. The test section was purpose-built, and the fuel slab and its supporter were slid into the test section through the gate (Fig. 2) when the inlet flow conditions were stable. In the ignition tests, the inlet gas velocity was 27 m/s, and the controlling parameters were the oxygen concentration (13–19%) and the inlet temperature (780–850°C). The error in the inlet temperature was less than ±4°C. The maximum uncertainty of the ignition delay determined by five tests of reproducibility was 7.3%.

The local regression of solid fuel was determined by measuring the variation of the thickness of the fuel slab after 400 s of heating under a hot flow stream. The details of the regression test were described by Yang and Wu.[8] The regression test, conducted with flow at 20 m/s and 700°C without oxygen added to the vitiator, ensured that no ignition occurred. The maximum uncertainty of the maximum fuel regression was 4.3%.

III. Results and Discussion

A. Flow Structure

Before investigating the ignition process, variations of the flow structure caused by the inlet configurations of backsteps were examined. The entry flow conditions and reattachment lengths corresponding to the five-step configurations are presented in Table 1, and the configurations of the five steps are sketched in Fig. 2. The boundary-layer thicknesses based on 99% of the freestream velocity were varied in the range 8.7–10.6 mm and the momentum thicknesses were 0.69–0.93 mm. The Reynolds number based on the momentum thickness ranged between 656–879. The shape factors (displacement thickness to momentum thickness) were 1.21–1.29. According to Pitz and Daily,[14] the shape factor of Blasius flow is about 2.4 and that of fully turbulent flow is about 1.3. The reattachment length of 7.7 step heights is consistent with a fully turbulent boundary layer as reported by Eaton and Johnston.[2] The value of momentum Reynolds number Re_θ is not consistent with a fully turbulent boundary layer. Eaton and Johnston showed that the reattachment length is not independent of Reynolds number (or in the fully turbulent regime) until Re_θ is about 1800. The boundary layer is transitional for Re_θ from 250 to 1800. In this work, Re_θ was about 800. The high turbulence level in the boundary layer (7%) may explain why the boundary layer appears turbulent at a low value of Re_θ.

The distributions of the horizontal and vertical mean velocities for the five step configurations are illustrated in Figs. 3 and 4, respectively; here X_r denotes the reattachment length

Table 1 Entry flow conditions and reattached flow characteristics at U_o = 15 m/s and T_o = 22°C

Inlet step configuration	Boundary-layer thickness, mm	Momentum thickness, θ, mm	Shape factor, H_{12}	Momentum Reynolds number, $U_o\theta/\nu$	T.I.[a]/U_o, %		Reattachment length, X/H	Maximum reverse flow rate, %
					Freestream	Boundary layer		
A	8.9	0.93	1.29	879	3.1	7.0	7.7	8.8
B	8.6	0.79	1.23	750	2.1	6.1	7.7	14.2
C	10.6	0.81	1.21	768	2.5	6.2	7.7	9.2
D	8.7	0.69	1.21	656	2.8	6.3	7.0	6.7
E	9.3	0.86	1.25	809	2.3	6.7	7.3	8.0

[a]Turbulence intensity.
Note: Uncertainty of reattachment length is less than 1.4%.

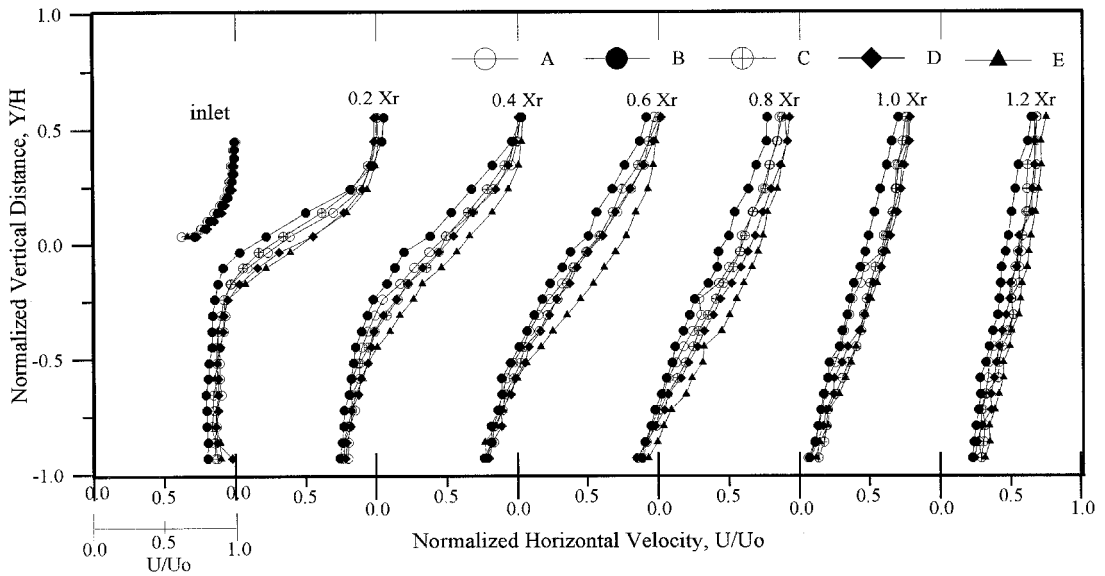

Fig. 3 Distributions of horizontal mean velocity with various steps.

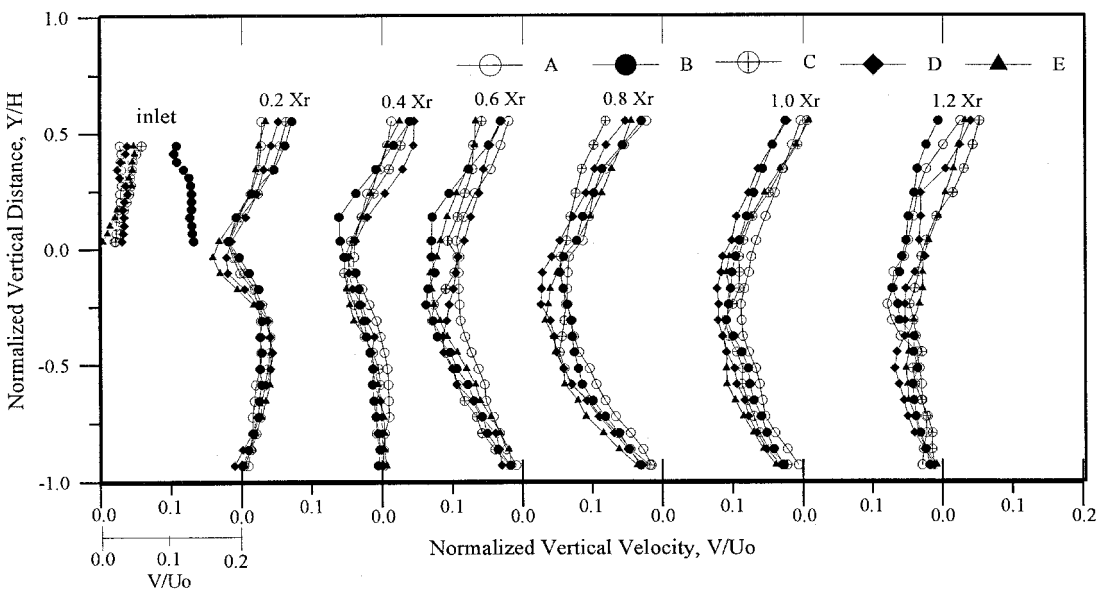

Fig. 4 Distributions of vertical mean velocity with various steps.

and the origin of the coordinate is at the separation point shown in Fig. 2. These velocities were normalized with the freestream velocity at the inlet U_o. The horizontal and vertical mean velocities above the separation point are not affected by the step, except that the convergent inlet of step B induced a relatively greater vertical velocity at the inlet (Fig. 4). Behind the backstep, the horizontal mean velocity of step B was the smallest and that of step E was the greatest, and the velocity deviation was augmented in the shear layer (Fig. 3). The vertical mean velocities of the five step configurations were scattered at each cross section of the combustor (Fig. 4).

The two-dimensional turbulence intensity, which denotes the mean kinetic energy of the turbulence per unit mass, is defined as

$$\text{turbulence intensity} = \left(\frac{\overline{u^2} + \overline{v^2}}{2}\right)^{1/2} \quad (1)$$

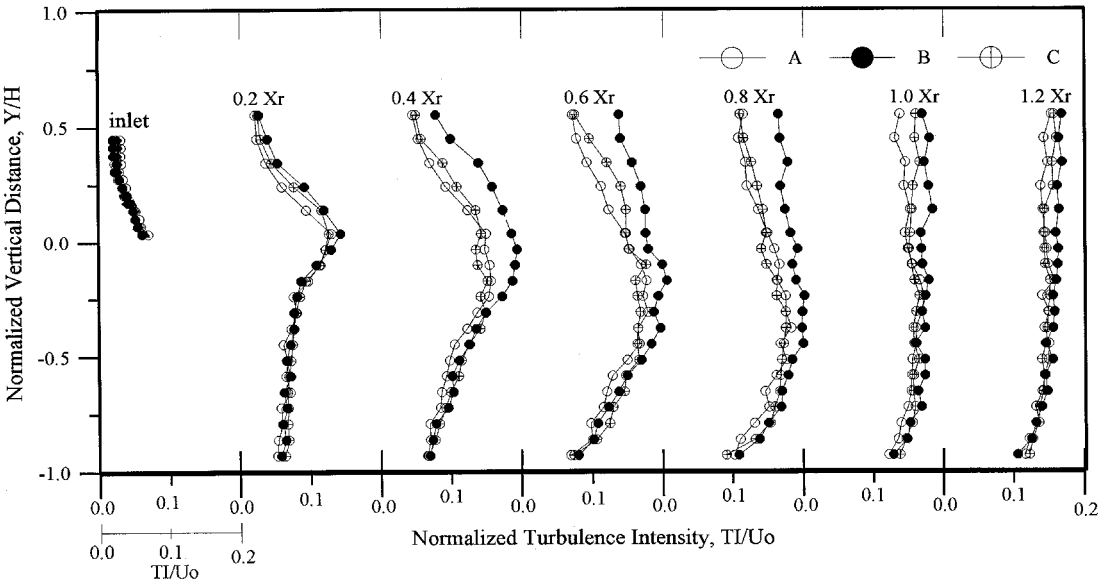

Fig. 5 Distributions of turbulence intensity with various steps.

where u and v are the fluctuations of the horizontal and vertical velocities, respectively. The turbulence levels measured in the boundary are very important in determining the reattachment length.[2] However, the measured levels may be artificially high due to velocity gradient broadening in the LDA probe volume.[9] Gradient broadening of the rms velocity is given by[9]

$$U_{rmsg} = \left[\frac{1}{4} d_y^2 \left(\frac{\partial U}{\partial y}\right)^2 + \frac{3}{64} d_y^4 \left(\frac{\partial U}{\partial y}\right)^4 + \cdots\right]^{1/2} \quad (2)$$

where d_y is the diameter of the probe volume in the y (gradient) direction. The curvature term is small throughout the flowfield, and the first term in Eq. (2) is important in the boundary layer at separation and in the shear layer. The gradient broadening given by Eq. (2) is subtracted from the turbulence intensity data reported here. Maximum corrections, about $0.008U_0$ at the inlet and $0.006U_0$ at $X/X_r = 0.2$, are much smaller than the values reported by Pitz and Daily.[9] The insignificant effects of the velocity gradient broadening might be caused by the high turbulent diffusion. The distributions of turbulence intensity at various cross sections behind the backstep depicted in Fig. 5 were similar to those in previous work of Driver and Seegmiller[15] and Yang et al.[16] The maximum value of turbulence intensity at each cross section increased monotonically from the separated point to a maximum at 0.6–0.8 reattachment length downstream from the step (see Fig. 6). Thereafter, the turbulence intensity decayed gradually. Only three curves of turbulence intensities for steps A, B, and C are shown in Fig. 5 in order to present a clear comparison of the differences among the three steps. The turbulence intensities at the inlet of the combustor for these three step configurations were almost identical, but the turbulence intensity in the combustor of step B was the greatest. The three distributions of turbulence intensity for steps A, B, and C converged gradually after $1.0X_r$. Figure 6 shows that the maximum turbulence intensity at each cross section behind step B was much greater than that behind other steps.

The reattachment length is defined as the point at which the average reverse flow velocity at 2 mm above the wall along the centerline of the combustor was zero. The reattachment lengths of steps A, B, and C were equal, whereas those of D and E were smaller (Table 1).

The streamlines in the combustor with various configurations of steps are depicted in Fig. 7, in which the horizontal coordinate is normalized with the reattachment length X_r. The

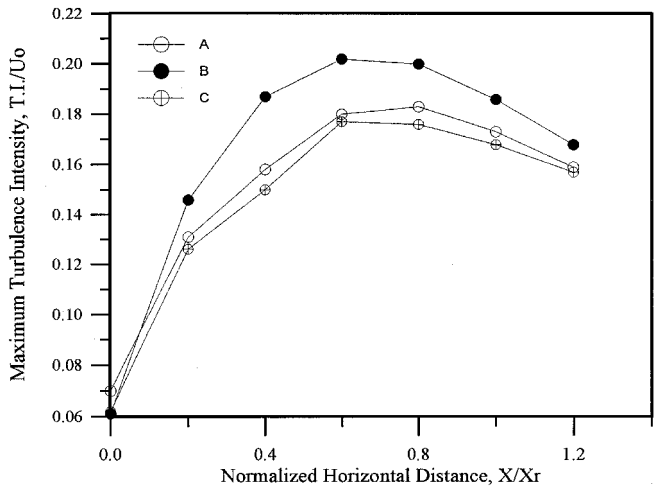

Fig. 6 Maximum turbulence intensities at various cross sections behind steps A, B, and C.

dividing streamlines, defined as the line of zero stream function, show that the width of the recirculation zone of step B was the greatest (35.2 mm), followed by step C (32.4 mm), whereas those of steps A, D, and E were 31.2, 29.5, and 29.7 mm, respectively. Evaluating varied shapes of the flameholder, Lefebvre[17] stated that the characteristic dimension of a bluff body should be not its geometric width, but the maximum width of the wake generated behind it. Therefore, the wider the recirculation zone, the more stable the flame. In our work, the width of the recirculation zone correlated well with the reverse flow rate.

In further investigation of flow features, a dimensionless local reverse flow rate is defined as

$$\frac{Q_r}{U_0 H} = \int_{-H}^{y^*} \frac{U_r \, dy}{U_0 H} \quad (3)$$

in which Q_r (m^3/s-m) is the reverse flow rate, U_r is the reverse flow velocity, U_0 the freestream velocity at the inlet, H the step height, and y^* corresponds to the point of zero horizontal velocity with negative horizontal velocity between $y = -H$ and y^*. The maximum reverse flow rates corresponding to the five steps appear in Table 1. Steps B and C generated the greatest reverse flow rates with values of 14.2 and 9.2%,

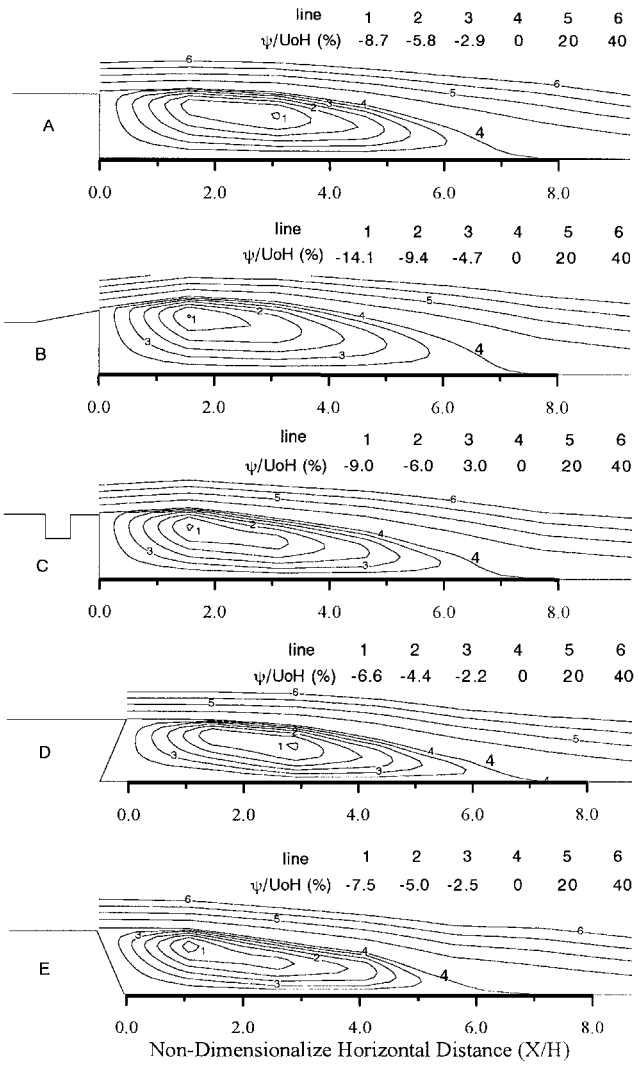

Fig. 7 Streamlines of flowfield behind various steps.

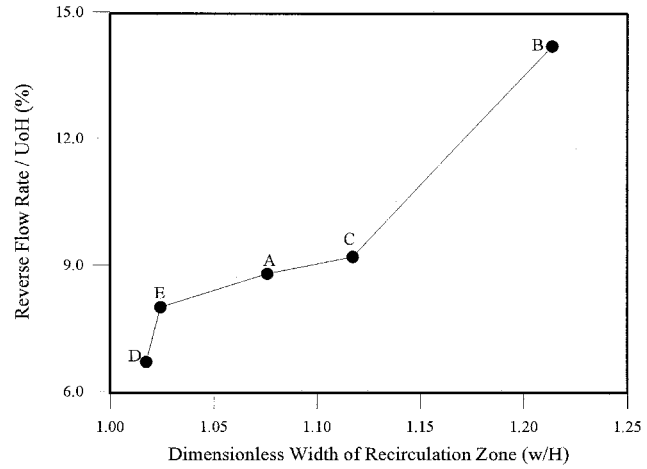

Fig. 8 Dimensionless reverse flow rate vs thickness of recirculation zone.

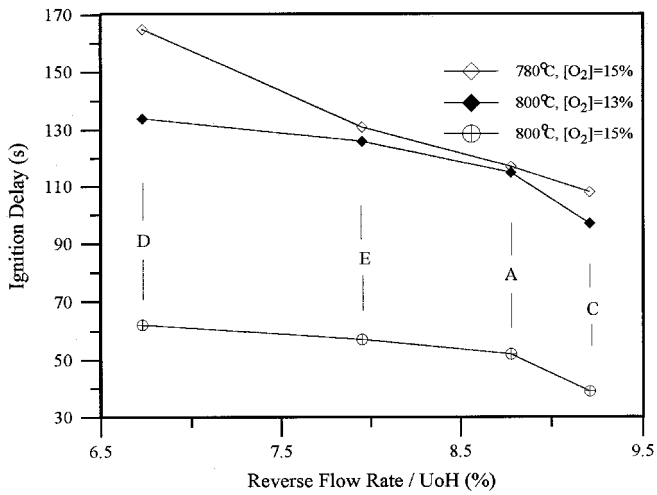

Fig. 9 Effect of reverse flow rate of cold gas on ignition delay for various inlet conditions.

respectively. The reverse flow rate increased with increasing width of the recirculation zone (Fig. 8): the relationship between rate of reverse flow and length of recirculation zone was less clear.

All evidence indicates that the effects of inlet configuration on the flow structure were significant in the recirculation zone and became small after the reattachment point. Steps B and C favorably increased the reverse flow rate, and step B generated the greatest turbulence intensity. As the flow structure in the recirculation zone is directly correlated with ignition and flame stabilization in a combustor, it is expected that proper modification of the inlet configuration will improve the combustion characteristics.

B. Ignition

The ignition test was performed in a hot flow. About 2 h were required to heat the flow stream to a stable and specified temperature, and the window of the test section was dusted by the seeding particles very quickly during the LDA measurement. These factors obstructed the LDA measurement in the hot flow. Although the turbulent features of hot flow in the ignition test might deviate slightly from those of cold flow, the trends of turbulent diffusion and the characteristics of flame stabilization are expected to be similar and the ignition phenomena can be interpreted from the aerodynamic data obtained from the cold flow.

After the fuel slab was slid into the test section containing a hot oxidizing gas stream, the surface of the solid fuel was elevated to the pyrolysis temperature. The pyrolyzed fuel vapor was then heated continuously and mixed with oxygen. Ignition occurred at the time and location at which the rate of the reaction reached a suitable accelerated condition; the entire process was monitored by a high-speed motion analyzer. At the beginning of ignition, one or several flame kernels initiated in the recirculation zone, followed by the development and spreading of individual kernels. Finally, all flame kernels joined to form a continuous flame zone. Photographs of the ignition process indicate the similarity of the ignition mechanisms in the five combustors.

The ignition delay is defined as the period between the time the fuel plate was slid into the test section and the first appearance of the flame. The ignition delays of five steps were tested under three inlet conditions of flow. The ignition delay decreased as the cold gas reverse flow rate increased (Fig. 9). Yang et al.[7] reported that high temperature and a large step height favored ignition, broadened ignition limits, and abbreviated ignition delay. In general, the flow for good flame stabilization abbreviates the ignition delay when the oxygen concentration is low. The large rate of reverse flow in this study provided good flame stabilization[6] and mixing of fuel and oxidizer in the recirculation zone, and hence, abbreviated ignition delay. Data for four reverse flow rates shown in Fig. 9 correspond to steps A, C, D, and E in Table 1. The ignition delay of step B did not fit this correlation (Fig. 9), possibly because of the intense turbulence behind step B. The turbulence inten-

sities behind steps A, C, D, and E varied little, but that behind step B was much greater. Although turbulent flow may enhance the mixing of fuel and oxidant, it also provided the least conducive conditions for ignition.[18] The ignition delay of step B was thus not the smallest, even though the rate of the reverse flow of step B was the largest.

Since steps B and C generated greater reverse flow rates and caused smaller ignition delays than the traditional step (A), the ignition delays of steps A, B, and C were investigated further. Figure 10 shows that the order of ignition delay was C < B < A when the oxygen concentration was less than 19%. When the oxygen concentration was increased to 19%, the variation of ignition delay with the various steps diminished.

Yang and Wu[19] depicted the ignition mechanism of solid fuel in the sudden-expansion combustor. When the oxygen concentration was less than 15%, the residence time of the mixture was important for the chemical reaction; hence, the initiated flame kernel of ignition was observed to occur within the recirculation zone due to its long residence time. When the oxygen concentration was higher than 20%, diffusion of fuel vapor into the oxidizing gas was the rate-controlling step; hence, the initiated flame kernel of ignition was observed to occur near the reattachment point and adjacent to the solid fuel due to rich fuel vapor there. The turbulence intensities, and hence, the turbulence diffusions of various steps near the reattachment point, were nearly the same (Fig. 5), so that the ignition delay was independent of the reverse flow rate of the cold gas at a high oxygen concentration.

Since the ignition process is generally controlled by the flow pattern when the oxygen content of the flow is small, ignition delay is significantly affected by variation of the inlet configuration of the combustor; modified steps B and C are expected to possess improved aerodynamic features for ignition and flame stabilization.

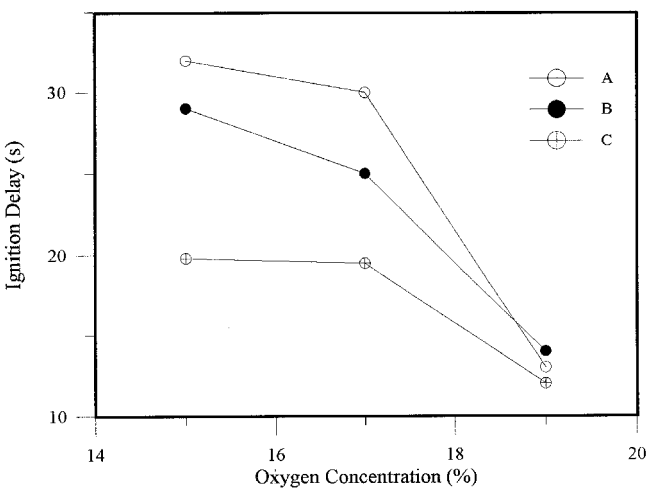

Fig. 10 Effect of oxygen concentration on ignition delay at temperature 850°C and velocity 27 m/s.

C. Fuel Regression

Investigating heat and mass transfer during the ignition process is important in understanding ignition, but is difficult due to transient phenomena. A feasible approach is to measure the regression of solid fuel in the hot flow stream without flame to simulate the phenomenon before ignition.[20] Therefore, the fuel regression defined in this work is different from the general definition given in previous work.[21–25]

The amount of local regression of solid fuel before ignition indicates the extent of heat transfer and fuel vapor pyrolyzed. In the profiles of local regression of solid fuel with five different steps at inlet velocity 20 m/s that appear in Fig. 11, the original thickness of the solid fuel was 10 mm. Local convective heat transfer increased gradually from just downstream of the inlet step to a maximum a few folds greater near the region of reattachment. Farther downstream, it decreased monotonically along the combustor, as reported by Zvulony et al.[25] The profiles of local regression of the solid fuel exhibited similar variations along the horizontal direction. The maximum regression was located 5.0–5.5 step heights from the inlet, which corresponds to the location of the reattachment point determined from the flame configuration after ignition.[7]

The combustor with a convergent inlet exhibited less regression within the recirculation zone. The smaller regression may have been caused by the thicker recirculation zone (Fig. 8), which inhibited heat transfer from the freestream to the surface of the solid fuel. This result is consistent with a previous study,[8] which showed that a large step height caused a small regression of solid fuel before ignition. However, in the region of the redeveloping boundary layer, the fuel regressions of these five combustors (Fig. 11) were nearly the same because the characteristics of flow and heat transfer in this region were no longer distinct.

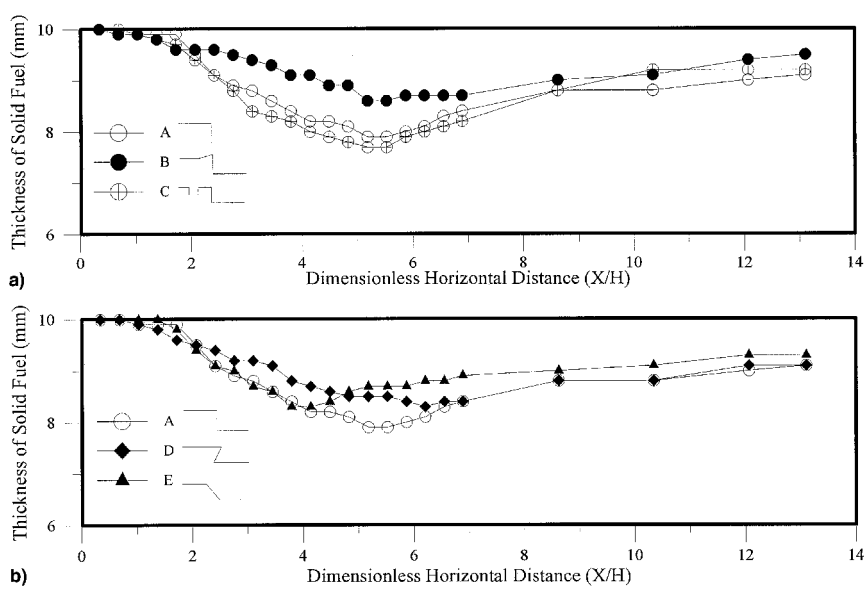

Fig. 11 Thickness of solid fuel slab at inlet velocity 20 m/s and temperature 700°C after heating for 400 s: a) steps A, B, and C and b) steps A, D, and E.

IV. Conclusions

The configuration of the inlet step had a notable effect on the turbulence intensity of the shear layer and the reverse flow rate of the recirculation zone, and less influence on the horizontal and vertical mean velocities behind the backstep. The convergent inlet of step B caused greater vertical velocity at the inlet and greater turbulence intensity in the shear layer behind the backstep. Compared to the traditional backstep (step A), reverse flow rates of modified steps B and C were larger and those of steps D and E were smaller. The rate of reverse flow increased with increasing width of the recirculation zone, but the length of the recirculation zone had a lesser relationship with the reverse flow rate.

Reverse flow rate, the major factor in shortening the ignition delay of the solid fuel, enhances the flameholding capability in the combustor. In general, the greater the reverse flow rate, the smaller the ignition delay. However, intense turbulence could compromise the effect of reverse flow rate on ignition delay because ignition favors slight turbulence if the flow is turbulent. Oxygen concentration is another important factor in ignition delay. When the oxygen concentration exceeded 19%, the effect of inlet configuration on ignition diminished and the ignition delays in the various configurations of steps were almost identical. Favorable design of the inlet port of a sudden-expansion combustor to improve ignition and flame stabilization involves generating a large rate of reverse flow without increasing turbulence intensity.

Acknowledgments

The authors thank Fang-Jinn Yang for assistance in the experiments, and the National Science Council of the Republic of China for support under Contracts NSC 82-0401-E-007-305 and NSC 83-0210-D-007-001.

References

[1]Etheridge, D. W., and Kemp, P. H., "Measurement of Turbulent Flow Downstream of a Rearward-Facing Step," *Journal of Fluid Mechanics*, Vol. 86, 1978, Pt. 3, pp. 545–566.

[2]Eaton, J. K., and Johnston, J. P., "A Review of Research on Subsonic Turbulent Flow Reattachment," *AIAA Journal*, Vol. 19, No. 9, 1981, pp. 1093–1100.

[3]Isomoto, K., and Honami, S., "The Effect of Inlet Turbulence Intensity on the Reattachment Process over a Backward-Facing Step," *Journal of Fluids Engineering*, Vol. 111, March 1989, pp. 87–92.

[4]Vogel, J. C., and Eaton, J. K., "Combined Heat Transfer and Fluid Dynamic Measurements Downstream of a Backward-Facing Step," *Journal of Heat Transfer,* Vol. 107, Nov. 1985, pp. 922–929.

[5]Sirka, V. P., Paujotas, P. M., and Zukauskas, A. A., "Characteristics of the Near Wake of a Cylinder in Crossflow," *Fluid Mechanics—Soviet Research*, Vol. 18, No. 4, 1989, pp. 13–22.

[6]Kundu, K. M., Banerjee, D., and Bhaduri, D., "On Flame Stabilization by Bluff-Bodies," *Journal of Engineering for Gas Turbines and Power*, Vol. 102, Jan. 1980, pp. 209–214.

[7]Yang, J.-T., Wu, C. Y. Y., and Din, S. J., "Ignition Transient of a Polymethylmethacrylate Slab in a Sudden Expansion Combustor," *Combustion and Flame*, Vol. 98, No. 3, 1994, pp. 300–308.

[8]Korting, P. A. O. G., Van der Geld, C. W. M., Wijchers, T., and Schoyer, H. F. R., "Combustion of Polymethylmethacrylate in a Solid Fuel Ramjet," *Journal of Propulsion and Power*, Vol. 6, No. 3, 1990, pp. 250–255.

[9]Elands, R., Dijkstra, F., and Zandbergen, B., "Experimental and Computational Flammability Limits in a Solid Fuel Ramjet," AIAA Paper 90-1964, July 1990.

[10]Schadow, K. C., Cordes, H. F., and Chieze, D. J., "Experimental Studies of Combustion Processes in a Tubular Combustor with Fuel Addition Along the Wall," *Combustion Science and Technology*, Vol. 19, 1978, pp. 51–57.

[11]Richardson, J., De Groot, W. A., Jagoda, J. I., Waiterick, R. E., Hubbartt, J. E., and Strahle, W. C., "Solid Fuel Ramjet Simulator Results: Experiment and Analysis in Cold Flow," *Journal of Propulsion and Power*, Vol. 1, No. 6, 1985, pp. 488–493.

[12]Schulte, G., Pein, R., and Hogl, A., "Temperature and Concentration Measurement in a Solid Fuel Ramjet Combustion Chamber," *Journal of Propulsion and Power*, Vol. 3, No. 2, 1987, pp. 114–120.

[13]Fernandez-Pello, A. C., Ray, S. R., and Glassman, I., *Eighteenth Symposium (International) on Combustion*, The Combustion Inst., Pittsburgh, PA, 1981, pp. 579–589.

[14]Pitz, R. W., and Daily, W., "Combustion in a Turbulent Mixing Layer Formed at a Rearward-Facing Step," *AIAA Journal*, Vol. 21, No. 11, 1983, pp. 1565–1570.

[15]Driver, D. M., and Seegmiller, H. L., "Features of a Reattaching Turbulent Shear Layer in Divergent Channel Flow," *AIAA Journal*, Vol. 23, No. 2, 1985, pp. 163–171.

[16]Yang, J.-T., Tsai, B. B., and Tsai, G. L., "Separated-Reattaching Flow over a Backstep with Uniform Normal Mass Bleed," *Journal of Fluids Engineering*, Vol. 116, No. 1, 1994, pp. 29–35.

[17]Lefebvre, A. H., *Gas Turbine Combustion*, Hemisphere, New York, 1983, p. 194.

[18]Kanury, A. M., *Introduction to Combustion Phenomena*, Gordon and Breach, New York, 1975, p. 126.

[19]Yang, J.-T., and Wu, C. Y. Y., "Controlling Mechanisms of Ignition of Solid Fuel in a Sudden-Expansion Combustor," *Journal of Propulsion and Power*, Vol. 11, No. 3, 1995, pp. 483–488.

[20]Yang, J. T., and Wu, C. Y. Y., "Solid Fuel Regression During Ignition Transient in a Ramjet," *Twenty-Fifth Symposium (International) on Combustion*, The Combustion Inst., Pittsburgh, PA, 1995, pp. 1603–1608.

[21]Elands, J. P. M., Korting, P. A. O. G., Wijchers, T., and Dijkstra, F., "Comparison of Combustion Experiment and Theory in Polyethylene Solid Fuel Ramjets," *Journal of Propulsion and Power*, Vol. 6, No. 6, 1990, pp. 732–739.

[22]Karadimitris, A., Scott, C., II, Netzer, D., and Gany, A., "Regression and Combustion Characteristics of Boron Containing Fuels for Solid Fuel Ramjets," *Journal of Propulsion and Power*, Vol. 7, No. 3, 1991, pp. 341–347.

[23]Netzer, A., and Gany, A., "Burning and Flameholding Characteristics of a Miniature Solid Fuel Ramjet Combustor," *Journal of Propulsion and Power*, Vol. 7, No. 3, 1991, pp. 357–362.

[24]Wooldridge, R. C., and Netzer, D. W., "Ignition and Flammability Characteristics of Solid Fuel Ramjets," *Journal of Propulsion and Power*, Vol. 7, No. 5, 1991, pp. 846–848.

[25]Zvulony, R., Gany, A., and Levy, Y., "Geometric Effects on the Combustion in Solid Fuel Ramjet," *Journal of Propulsion and Power*, Vol. 5, No. 1, 1989, pp. 32–37.